TASK QUARTERLY 5 No 4 (2001), 519–535

NUMERICAL CALCULATION OF THE STEAM CONDENSING FLOW

SŁAWOMIR DYKAS

Institute of Power Machinery,
Silesian Technical University,
Konarskiego 18, 44-100 Gliwice, Poland
dykas@rie5.ise.polsl.gliwice.pl

(Received 28 June 2001; revised manuscript received 14 August 2001)

Abstract: Considering the flow in the last stages of LP (low pressure) steam turbine the strong non-linearity of the thermal parameters of state and possibility of the two-phase flow have to be taken into account in the numerical calculation of the flow field. In this paper numerical calculations of the steam condensing flow for the turbine geometry are presented. The steam properties are described here on the basis of the IAPWS'97 formulation. The classical nucleation theory of Volmer and Frenkel was adapted for modelling of condensing flow. The droplet growth model of Gyarmathy is implemented. The calculations are based on the time dependent 3D Euler equations, which are coupled to three additional mass conservation equations for the liquid phase and are solved in conservative form.

Keywords: condensation, homogeneous, heterogeneous, real gas, wet steam

Nomenclature

c [m/c] – speed of sound
c_p [J/(kgK)] – specific heat capacity at constant pressure
c_v [J/(kgK)] – specific heat capacity at constant volume
e [J/kg] – specific density energy
h [J/kg] – specific enthalpy
J_{hom} [$m^{-3}s^{-1}$] – nucleation rate per unit volume of mixture
Kn – Knudsen number
L [J/kg] – latent heat
m [kg] – mass of water molecule
n_{het} [m^{-3}] – concentration of impurities
n_{hom} [kg^{-1}] – concentration of droplets
p [Pa] – static pressure
Pr – Prandtl number
R [J/(kgK)] – individual gas constant
r^* [m] – Kelvin-Helmholtz critical radius
r_{het} [m] – particle radius
r_{hom} [m] – droplet radius
s [J/(kgK)] – specific entropy
T [K] – static temperature
v [m^3kg] – specific volume

y_{hom} [kg/kg] – homogeneous wetness fraction
y_{het} [kg/kg] – heterogeneous wetness fraction
z – coefficient of compressibility
ΔT [K] – subcooling
α_c – condensation coefficient
γ – isentropic exponent
λ [W/(mK)] – thermal conductivity of vapour
ρ [kg/m^3] – density
σ [N/m] – surface tension of wather

SUBSCRIPTS:
l – liquid phase
g – gas phase
s – saturation state

1. Introduction

The numerical calculation of flow in LP steam turbines is a very important and difficult issue. European power industry is based to a large degree on fossil fuels. The older power plants, which are approaching the end of their lifetime, must be completely retrofitted and upgraded. Also the environmental question must be taken into account: optimum use of the available fuels, ensuring highest possible efficiency, combined with the reduction of the ecologically harmful emissions to an absolute minimum. It is obvious that great efforts should be focused not only on the increase of the thermal efficiency of the power plants by raising the live steam parameters but also on reducing the losses in the turbine.

Since significant part of the total net power output of a power plant is produced in the LP steam turbine, accurate modelling and computation of the flow through the LP steam turbine stages is of great technical and economical importance. Steam turbines are used worldwide by the electrical power supply industry and it is imperative that their turbines are of the highest cycle efficiency, since a small increase in efficiency can result in huge amount being saved over the lifetime of the machine. The condensing LP steam turbines are the most expensive element of both fossil-fired and nuclear power plant turbines. Many factors are involved here, *e.g.* the operation in the two-phase regime (two types of nucleation exist here: spontaneous and heterogeneous) and the extremely 3D flow due to the rapid increase of the steam volume as a result of expansion. The liquid phase in the flow through the turbine stages contributes to the severe erosion of the blades. An ability to predict the steam condensing flow through the last stages of the LP turbine allows one to determine the losses and suggests how to minimise them.

Because of the 3D complex nature of flow in LP turbine stages, the reproduction and measurement of this flow in a laboratory is very difficult and expensive. Therefore, the numerical investigation of these types of flows is very important. It is necessary to emphasise that in reality turbine condensation is determined by the conditions which are different, compared to the nozzle flow.

Condensation in wet steam flows has been numerically investigated by, among others, Hill [1], Bakhtar [2], Deyc [3], Stastny [4, 5]. These authors have mainly concentrated on 2D steady flow of nucleating steam in single cascades. Schnerr [6, 7] investigates numerically unsteady turbulent multiphase 2D flows through whole stages with homogeneous and heterogeneous condensation. All these methods are based on the classical nucleation theory of Volmer and Frenkel [8].

The flow through the last stages can not be approximated using 2D calculations, because of the extremely 3D character of this flow. The 3D calculations are necessary, in spite of the noticeable increase of the computational time. The development of the numerical methods, computer science, and technology allows one to calculate more complex flows.

2. Flow model

2.1. Governing equations

Wet steam is assumed to be a mixture of vapour at pressure p, temperature T_g and density ρ_g, and liquid phase at the same pressure, temperature T_l and density ρ_l. The liquid phase consists of large numbers of spherical liquid droplets of various sizes (radius r). The wetness fraction y is given by:

$$y = \frac{4}{3} \cdot \pi \cdot r^3 \cdot \rho_l \cdot n \tag{1}$$

and mixture density ρ by:

$$\rho = \frac{\rho_g}{(1-y)}. \tag{2}$$

The mixture specific internal density energy e can be expressed as:

$$e = \left((1-y) \cdot e_g + y \cdot e_l\right) \cdot \rho, \tag{3}$$

where $y = y_{hom} + y_{het}$.

Neglecting the interface velocity slip, the governing equations in conservative form for the inviscid compressible flow can be written in the following way:

$$\frac{\partial}{\partial t}\begin{Bmatrix} \rho \\ \rho \cdot u \\ \rho \cdot v \\ \rho \cdot w \\ E \\ \rho \cdot y_{hom} \\ \rho \cdot n_{hom} \\ \rho \cdot y_{het} \end{Bmatrix} + \frac{\partial}{\partial x}\begin{Bmatrix} \rho \cdot u \\ \rho \cdot u^2 + p \\ \rho \cdot u \cdot v \\ \rho \cdot u \cdot w \\ u \cdot (E+p) \\ \rho \cdot u \cdot y_{hom} \\ \rho \cdot u \cdot n_{hom} \\ \rho \cdot u \cdot y_{het} \end{Bmatrix} + \frac{\partial}{\partial y}\begin{Bmatrix} \rho \cdot v \\ \rho \cdot v \cdot u \\ \rho \cdot v^2 + p \\ \rho \cdot v \cdot w \\ v \cdot (E+p) \\ \rho \cdot v \cdot y_{hom} \\ \rho \cdot v \cdot n_{hom} \\ \rho \cdot v \cdot y_{het} \end{Bmatrix} + \frac{\partial}{\partial z}\begin{Bmatrix} \rho \cdot w \\ \rho \cdot w \cdot u \\ \rho \cdot w \cdot v \\ \rho \cdot w^2 + p \\ w \cdot (E+p) \\ \rho \cdot w \cdot y_{hom} \\ \rho \cdot w \cdot n_{hom} \\ \rho \cdot w \cdot y_{het} \end{Bmatrix} =$$

$$= \begin{Bmatrix} 0 \\ 0 \\ 0 \\ 0 \\ 0 \\ \frac{4}{3} \cdot \pi \cdot \rho_l \cdot \left(J_{hom} \cdot r^{*3} + 3 \cdot \rho \cdot n_{hom} \cdot r_{hom}^2 \cdot \frac{dr_{hom}}{dt} \right) \\ J_{hom} \\ 4 \cdot \pi \cdot \rho_l \cdot n_{het} \cdot r_{het}^2 \frac{dr_{het}}{dt} \end{Bmatrix} \tag{4}$$

where

$$E = e + \rho \cdot \frac{1}{2}\left(u^2 + v^2 + w^2\right). \tag{5}$$

The governing Euler equations for the vapour phase are coupled with three additional mass conservation equations for the liquid phase and are solved in conservative form.

The mathematical closure of these equations requires knowledge of the equation of state for steam and separate equation for wetness fractions. The homogeneous wetness fraction is obtained from the theories of nucleation and droplet growth. Heterogeneous effects are simulated by assuming a given concentration of spherical particles of impurities

$n_{het,0}$ per cubic meter with a given radii $r_{het,0}$, where the liquid mass can grow according to the droplet growth law applied, *i.e.* neglecting preceding nucleation on the particle surface [7].

2.2. Equation of state

Steam in superheated and supersaturated state departs appreciably from ideal gas laws. The adaptation of the real gas equations of state to the numerical solution of the governing equations causes significant increase of the computational time, *e.g.* implementation of the fundamental equation of state (IAPWS-IF 97) [9] increases the computational time 90 times and the implementation of the virial equation of state with three virial coefficients (Vukalovich's equation of state [10]) 8 times. In the present calculations the "local" real gas equation of state was implemented. This increases the computational time only 3 times in comparison with the ideal equation of state (Table 1).

Table 1. Comparison of calculation time for the various equations of state

Equation of state	Form	Factor
ideal gas	$\frac{p\cdot v}{R\cdot T} = 1 + B(T)\cdot\frac{1}{v} + C(T)\cdot\frac{1}{v^2} + D(T)\cdot\frac{1}{v^3}$	1
"local" real gas	$\frac{p\cdot v}{R\cdot T} = 1$	~ 3
Vukalovich	$\frac{p\cdot v}{R\cdot T} = A(T) + B(T)\cdot\frac{1}{v}$	~ 8
IAPWS-IF 97	$\frac{g(p,T)}{R\cdot T} = \gamma(\pi,\tau) = \gamma(\pi,\tau)^0 = \gamma(\pi,\tau)^r$	~ 90

The mathematical form of the "local" real gas equation of state is similar to the virial equation of state with one virial coefficient:

$$\frac{p\cdot v}{R\cdot T} = z(T,v) = A(T) + B(T)\cdot\frac{1}{v}, \tag{6}$$

where $A(T)$ and $B(T)$ are the polynomials, whose coefficients are determined on the basis of approximations of the fundamental equation of state (IAPWS'97). These polynomials play a role of the virial coefficients.

Equation of state (6) is valid for the limited range of steam parameters and its coefficients must be determined every time for the considered flow conditions (Figure 1). The degree of these polynomials increases together with the area of validity of "local" equations of state. Due to the application of the very accurate state equation for real gas (IAPWS-IF 97) to the calculation of the thermodynamic properties of steam, the thermodynamic properties and the flow kinematic is calculated accurately.

Because of application of the state equation for real gas as a supplementary equation for the governing Equation (4), the calculation of the pressure from Equation (5) becomes much more complicated than in the case of state equation for real gas. This is the main reason for the increase of computational time.

Expressions for enthalpy, entropy and other properties are determined here from usual thermodynamic relationships [11]:

$$h = h_0 + \Delta h, \tag{7}$$

$$s = s_0 + \Delta s, \tag{8}$$

$$c_p = c_{p_0} + \Delta c_p, \tag{9}$$

$$c_v = c_{v_0} + \Delta c_v. \tag{10}$$

The relations for the referential state can be assumed according to Vukalovich [10].

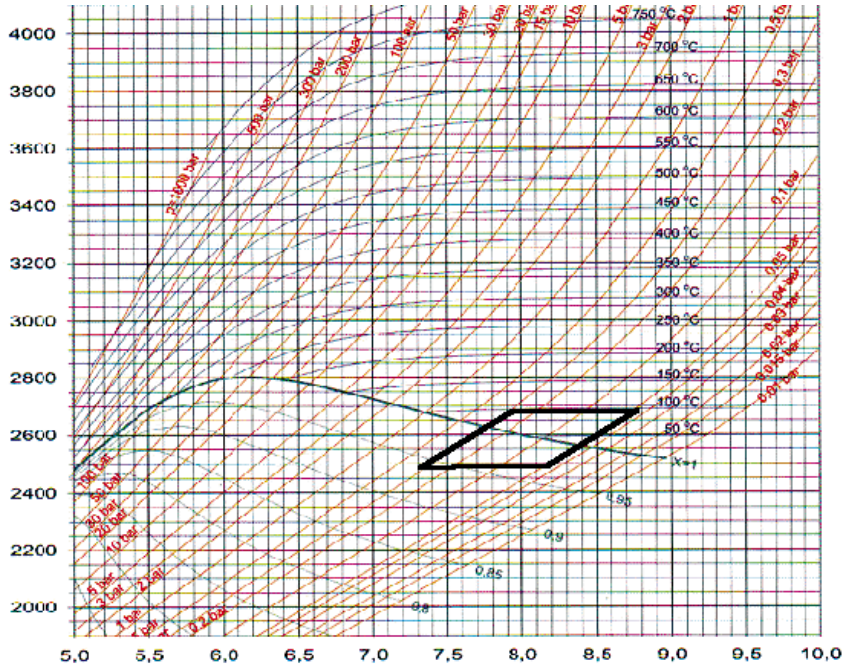

Figure 1. h-s diagram for steam with a marked area of validity of the "local" equation of state

The enthalpy departures Δh are related to the equation of state by the following equation:

$$\Delta h = R \cdot T \int_0^{\rho} \left(\frac{\partial z}{\partial T} \right)_{\rho} \frac{d\rho}{\rho} + R \cdot T \cdot (1 - z), \tag{11}$$

similarly for entropy:

$$\Delta s = R \int_0^{\rho} \left(\frac{z_T - 1}{\rho} \right) d\rho + R \cdot \ln(\rho \cdot R \cdot T), \tag{12}$$

specific heat capacity at constant volume:

$$\Delta c_v = R \cdot T \int_0^{\rho} \left(\frac{\partial z_T}{\partial T} \right)_{\rho} \frac{d\rho}{\rho} \tag{13}$$

and pressure:

$$c_p - c_v = R \frac{z_T^2}{z_v}. \tag{14}$$

In the above Equations (11)–(14), besides the equation of state, the following expressions must be known:

$$z_T(T, v) = z + T \cdot \left(\frac{\partial z}{\partial T} \right)_v \text{ and } \quad z_v(T, v) = z - v \cdot \left(\frac{\partial z}{\partial v} \right)_T. \tag{15}$$

Also the speed of sound and the isentropic exponent are determined in the same way:

$$c^2 = R \cdot T \cdot \left(\frac{R}{c_v} \cdot z_T^2 + z_v \right), \tag{16}$$

$$\gamma = \frac{1}{z} \cdot \left(\frac{R}{c_v} \cdot z_T^2 + z_v \right). \tag{17}$$

The concept of the "local" real gas equation of state can be applied to determine the thermodynamic properties of the real gas, in the case when the simple mathematical form is necessary.

2.3. Classical nucleation theory

The rate of formation of droplets due to the spontaneous condensation per unit volume of the mixture is obtained from the classical theory of non-isothermal homogeneous condensation:

$$J_{hom} = C \cdot \sqrt{\frac{2 \cdot \sigma}{\pi}} \cdot m^{\frac{3}{2}} \cdot \frac{\rho_g^2}{\rho_l} \cdot e^{\beta \cdot \left(-\frac{4 \cdot \pi \cdot r^{*3} \cdot \sigma(T)}{3 \cdot R \cdot T_g} \right)}, \tag{18}$$

where C is a non-isothermal correction factor proposed by Kantrowitz [12]. The coefficient β, proposed by Deyc [3], obtained on the basis of many experiments, plays a role of the correction factor (Gibbs free energy correction factor). In the present paper this factor is neglected (set to one). But other authors, besides of course Deyc and Fillipov [3], such as Stastny [4, 5] use this factor to obtain precise agreement with experimental data. This coefficient strongly depends on the pressure at the starting point of spontaneous nucleation.

A very important term in the estimation of nucleation rate is the surface tension σ. The value of σ can be calculated from the relation proposed by Deyc [3]. In this work, only the variations of σ with the temperature are taken into account:

$$\sigma(T) = \begin{cases} 138^{-3} - 0.212^{-3} \cdot T, & T \geq 373.15\,\mathrm{K}, \\ 122^{-3} - 0.17^{-3} \cdot T, & T < 373.15\,\mathrm{K}. \end{cases} \tag{19}$$

The Kirkwood-Buff equation can be used to relate the surface tension to the radius of curvature as follows:

$$\frac{\sigma(T,r)}{\sigma(T)} = \frac{1}{1 + 2 \cdot \frac{10^{-10}}{r}}, \tag{20}$$

but the above relation arouses large uncertainty.

2.4. Critical droplet size

The vapour pressure of the convex liquid surface is larger than that of a plane one, according to the relation:

$$p_l = p_g + p_\sigma = p_g + \frac{2 \cdot \sigma(T)}{r}. \tag{21}$$

If the drop is surrounded by supersaturated vapour atmosphere, with known supersaturation ratio (S) or subcooling (ΔT), there is an unstable droplet, called "critical droplet", which can evaporate or grow, depending on the conditions.

The size of the "critical droplet" is determined from the equality of chemical potentials for the gas and liquid phase, as follows:

$$r^* \rightarrow dg(p,v)_g|_{T=const.} = dg(p,v)_l|_{T=const.}, \tag{22}$$

$$g_g(p_g, v_g) = v_g dp_g, \tag{23}$$

$$g_l(p_l, v_l) = v_l dp_l = v_l dp_g + v_l d\left(\frac{2 \cdot \sigma(T)}{r} \right), \tag{24}$$

$$v_g dp_g = v_l dp_g + v_l d\left(\frac{2 \cdot \sigma(T)}{r} \right), \tag{25}$$

$$v_g dp_g - v_l dp_g = v_l d\left(\frac{2\cdot\sigma(T)}{r}\right). \tag{26}$$

Substituting v_g determined from the "local" gas equation of state (6) to Equation (26) and after integration (left side from p_s to p_g and right side from $r \to \infty$ to r^*) we will obtain the expression for the Kelvin relation for the size of the critical droplet compatible with the "local" real gas equation of state.

2.5. The growth of the droplet radius

Nuclei that emerge from the nucleation process as supercritical stable droplets will further grow by condensation of the vapour on their surface. Coagulation is generally thought to play an unimportant role in nozzles and LP turbine flow. The rate of condensation on a drop is governed by the rate at which latent heat L can be carried away from the surface into the cooled vapour. The relative velocity between droplet and vapour is here neglected (no-slip conditions), and the droplet is assumed to be spherical and surrounded by an infinite vapour space.

The heat transferred in a unit time from the droplet to the surrounding vapour is expressed as:

$$\dot{Q} = 4\cdot\pi\cdot r^2\cdot\alpha\cdot\left(T_l - T_g\right) \tag{27}$$

and is equal to the liberation latent heat:

$$\dot{Q} = L\cdot\frac{dm}{dt} = L\cdot 4\cdot\pi\cdot r^2\cdot\rho\cdot\frac{dr}{dt}. \tag{28}$$

The heat capacity of the droplet is negligible due to the low heat.

Thus the equation of droplet growth can be expressed as:

$$\frac{dr}{dt} = \frac{\alpha}{\rho_l}\cdot\frac{T_l - T_g}{L}. \tag{29}$$

α is heat transfer coefficient of the sphere. For the liquid/vapour interaction, α can be expressed as:

$$\alpha = \frac{\lambda_g}{r}\cdot\frac{1}{\left(1+(1-v)\cdot\dfrac{2\cdot\sqrt{8}\cdot\pi}{1.5}\cdot\dfrac{\gamma}{\gamma+1}\cdot\dfrac{\mathrm{Kn}}{\mathrm{Pr}_g}\right)}. \tag{30}$$

In Equation (30) the factor v is a semiempirical correction factor which is included to obtain precise agreement with droplet size measurements in LP nozzle experiments. This factor was proposed by Young, developed by White and Young [13–15] and can be determined from the expression:

$$v = \frac{RT_s(p)}{L}\cdot\left[\alpha_{ce} - 0.5 - \frac{2-\alpha_c}{2\alpha_c}\cdot\left(\frac{\gamma+1}{2\gamma}\right)\cdot\frac{c_p T_s(p)}{L}\right], \tag{31}$$

where α_{ce} is a constant, which relates the condensation and evaporation coefficient.

In the presented calculations the factor v equals zero. It must be emphasised that for this assumption the droplets size is almost always less than the measured value (if another correction is not used, *i.e.* correction of the nucleation rate). However, the calculated wetness fraction is very close to the measured value. Smaller droplet radii cause the increase of their concentration.

The heat transfer is driven by a temperature difference $T_l - T_g$. The surface temperature of the droplet depends also on its radius. For large sizes ($r \gg r^*$) the temperature

T_l approaches saturation temperature $T_s(p)$. When the sizes are close to the critical size ($r \approx r^*$), the temperature of the droplet approaches the temperature of the gas phase (vapour) T_g. The temperature T_l is thus given by:

$$T_l = T_s(p) - \left(T_s(p) - T_g\right) \cdot \frac{r^*}{r} = T_s(p) - \Delta T \cdot \frac{r^*}{r}. \tag{32}$$

3. Numerical results

The algorithm used to solve the system of governing Equation (4) is a time-marching Godunov-type method [16] coupled with the solution of the differential equations for the liquid phase. The discretization in space is based on the cell-centered finite volume method. The explicit, first-order accurate forward time integration is implemented.

Values of the numerical fluxes on the cell surfaces are calculated from the exact solution of the local one-dimensional Riemann problems for the real gas equation of state (6).

The classical Godunov scheme leads to monotonic algorithm of the first-order accuracy in space. To obtain higher accuracy and preserve monotonicity, the van Leer's MUSCL approximation has been applied with van Albada's limiter function [17, 18].

The numerical calculations can be split into two groups. First, the comparative numerical calculations. The numerical results are compared with experimental data or other calculations. These calculations serve as a test for numerical algorithm, its correctness in the modelling of the physical phenomena. The second group of numerical calculations are the calculations in which we can not link our results to exact laboratory measurements or to other calculations. In this case, very valuable is knowledge about the calculated physical phenomenon and the ability to draw conclusions from the previous calculations (experience).

The method developed has been applied to several test cases. Some of them are given below, such as the comparative numerical calculations of 2D condensing flow and 3D flow through the stator of the last stage LP 200 MW steam turbine.

3.1. Nozzle flow calculations

3.1.1. Homogenoeus condensation in the Barschdorff nozzles

Among many test cases carried out to check the correctness of modelling the condensing flow, the expansion in the Barschdorff nozzle was presented. This nozzle is an arc nozzle with the critical throat height 60 mm and radius of the wall curvature 584 mm. The calculations were done for the two initial parameters, first, total pressure $p_0 = 0.0785$ MPa and temperature $T_0 = 380.55$ K and second, total pressure $p_0 = 0.0785$ MPa and temperature $T_0 = 373.15$ K. The numerical results were compared with experiment and other numerical calculations [19]. The obtained results, presented in Figures 2 and 3 show good agreement with experimental measurements of pressure distribution and with other calculations of pressure and droplet radius distributions.

3.1.2. Heterogenoeus condensation in the Barschdorff nozzle

The influence of concentration of impurities $n_{het,0}$ of radius $r_{het,0} = 10^{-8}$ m on transonic flow of steam through the arc nozzle was investigated (the critical throat height was 60 mm, and radius of the wall curvature 584 mm). Calculations were done for the total pressure $p_0 = 0.0785$ MPa and temperature $T_0 = 380.55$ K. Figures 4, 5, 6 and 7 show the relation of the homogeneous nucleation rate $\log_{10}(J_{hom})$ and static pressure ratio p/p_0 of the adiabatic

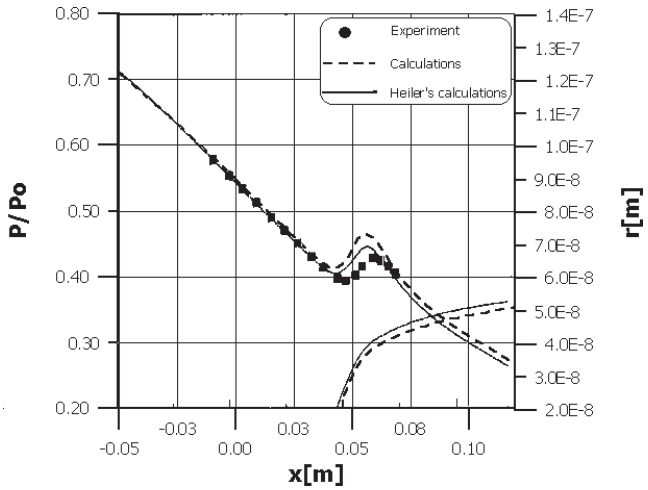

Figure 2. Pressure ratio and droplet radius distribution ($p_0 = 0.0785\,\mathrm{MPa}$, $T_0 = 380.55\,\mathrm{K}$)

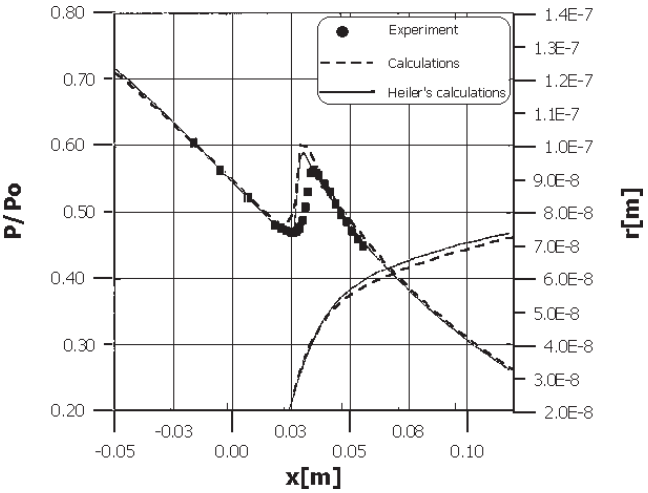

Figure 3. Pressure ratio and droplet radius distribution ($p_0 = 0.0785\,\mathrm{MPa}$, $T_0 = 373.15\,\mathrm{K}$)

and diabatic flow. The homogeneous, and heterogeneous wetness fraction along the nozzle axis are depicted on the right hand side of these figures.

A stepwise increase of the particle number concentration leads to a significant change in the flow pattern. The concentration of 10^{14} particles per cubic meter did not change the flow pattern in any significant way (Figure 5) in comparison with the homogeneous flow (Figure 4). In the case of concentration $10^{15}\,\mathrm{m}^{-3}$, the heterogeneous wetness fraction increases. It weakens the homogenous condensation and moves the increase of the pressure downstream (Figure 6). For the concentration $10^{16}\,\mathrm{m}^{-3}$, due to the subsonic heat addition ahead of the nozzle throat, the supersonic compression typical for the homogeneous condensation disappears (Figure 7).

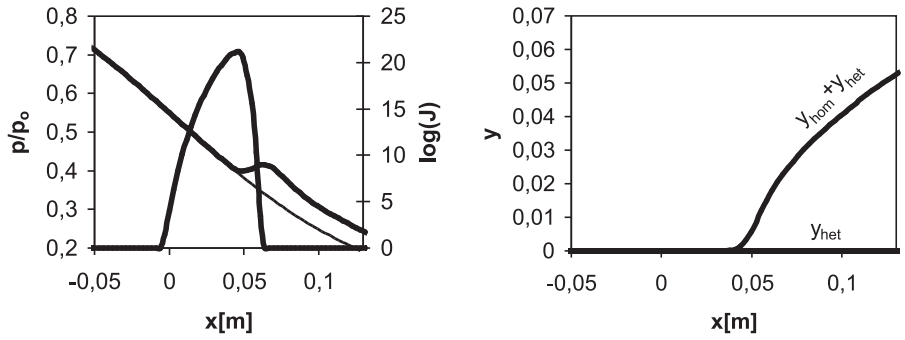

Figure 4. Distribution of the flow parameters for the homogeneous flow

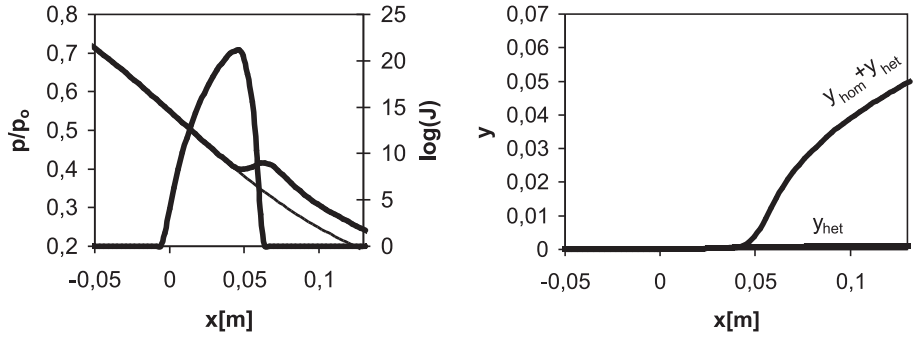

Figure 5. Distribution of the flow parameters for the heterogeneous flow ($n_{het,0} = 10^{14}\,\mathrm{m}^{-3}$, $r_{het,0} = 10^{-8}\,\mathrm{m}$)

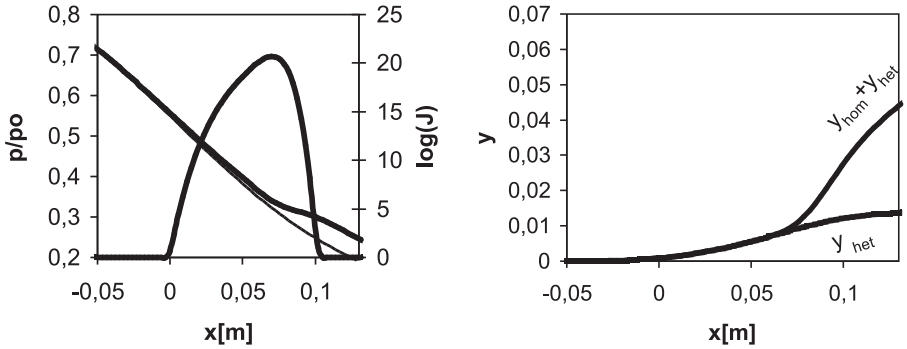

Figure 6. Distribution of the flow parameters for the heterogeneous flow ($n_{het,0} = 10^{15}\,\mathrm{m}^{-3}$, $r_{het,0} = 10^{-8}\,\mathrm{m}$)

3.2. Turbine cascade flow calculations

3.2.1. 2D condensing flow

The blade cascade considered in the test case is the fifth stage stator blade from the six stage LP cylinder of a 600 MW turbine. The design exit Mach number is 1.2 and the outlet flow angle is about 71°. The performance of this cascade, test data from experiments and predictions were reported by White *et al.* [15]. In the present paper the so-called L-1 condition of the water steam flow is considered. The L-type tests represent a low inlet superheat (4.5 – 7.5 K).

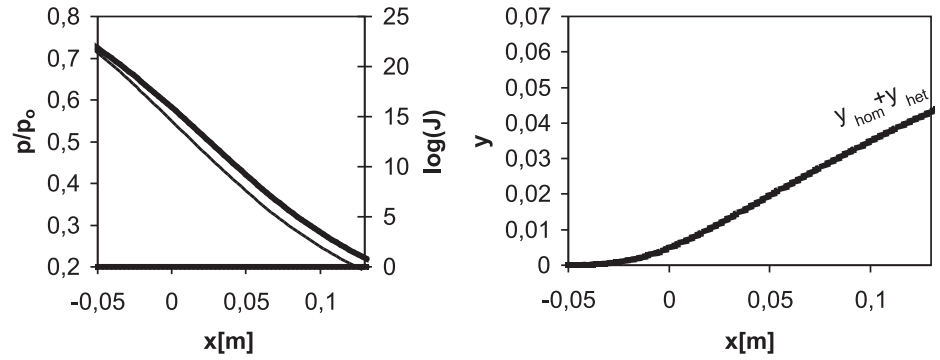

Figure 7. Distribution of the flow parameters for the heterogeneous flow ($n_{het,0} = 10^{16}\,\mathrm{m}^{-3}$, $r_{het,0} = 10^{-8}\,\mathrm{m}$)

The calculation domain was discretised with an "I"-type, orthogonal grid. The discretization was constructed using 356×51 nodes with lines adjusted to the expected direction of condensation shock so as to minimise the numerical error. For this type of grid, a modification of periodic boundary conditions at the outlet was necessary. The trailing edge of the profile used in the calculations was slightly sharpened to eliminate blunt trailing edge making difficulties in the inviscid flow calculations. The Mach number and pressure contours for the L-1 test are presented in Figures 10 and 11. The increase of the static pressure caused by the heat addition process is more rapid than in the experiment (Figure 8).

Table 2. Boundary conditions for flow in the turbine cascade

Test	Inlet stagnation pressure p_0 [kPa]	Inlet stagnation temperature T_0 [K]	Outlet static pressure p_2 [kPa]
L-1	40.3	354	16.3

The averaged droplet radius calculated at the outlet at a distance of 18% of the chord length downstream of the trailing edge was compared with measurements [15] (Figure 9). The differences in radii are visible in this case. The droplet growth model causes these differences. In these calculations no experimental correction factors were used as in contrast to the calculations performed in [15]. The averaged wetness fraction obtained in the calculations is $y = 0.33$ and is very close to the experimental one $y_{exp} = 0.34$.

The differences between the outlet angle obtained in the adiabatic and diabatic calculations were observed. The angles differ by about 2.5° (Figure 12). The cascade loss coefficient was calculated from the formula:

$$\zeta = \frac{T_2 \Delta s}{\frac{1}{2} c_2^2}, \tag{33}$$

where T_2 is the outlet temperature, Δs is entropy production and c_2 is velocity at the outlet. In the loss coefficient calculations from the measurements, the viscous losses were excluded. Calculated loss coefficients were predicted about 1% greater than in the measurements.

3.2.2. 3D condensing flow

Calculations of 3D steam condensing flow through a turbine stator cascade were performed. The geometry of the last stage LP steam turbine stator was chosen (Figure 13).

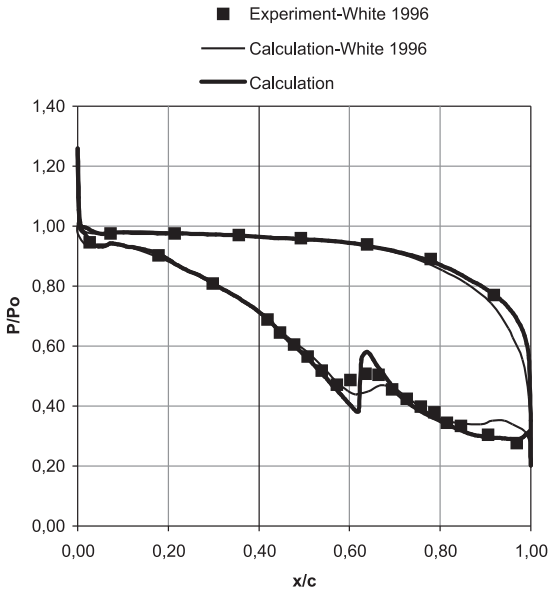

Figure 8. Distribution of the pressure on the profile

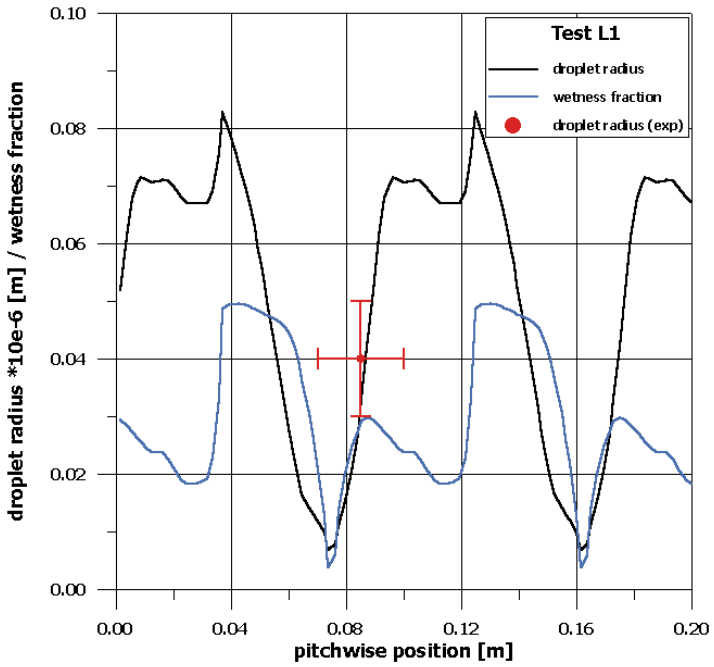

Figure 9. Distribution of the radius and wetness fraction along the pitch

These calculations were carried out with the following inlet parameters: $p_0 = 0.145\,\text{bar}$, $\rho_0 = 0.076\,\text{kg/m}^3$. The outlet pressure at the mid-span was $p_{out} = 0.07\,\text{bar}$.

According to the theory of radial equilibrium, the outlet pressure increases from the blade hub (blade root) to blade tip, preserving the fixed outlet pressure at the mid-span. Therefore the maximum expansion is close to the blade hub. There are suitable conditions

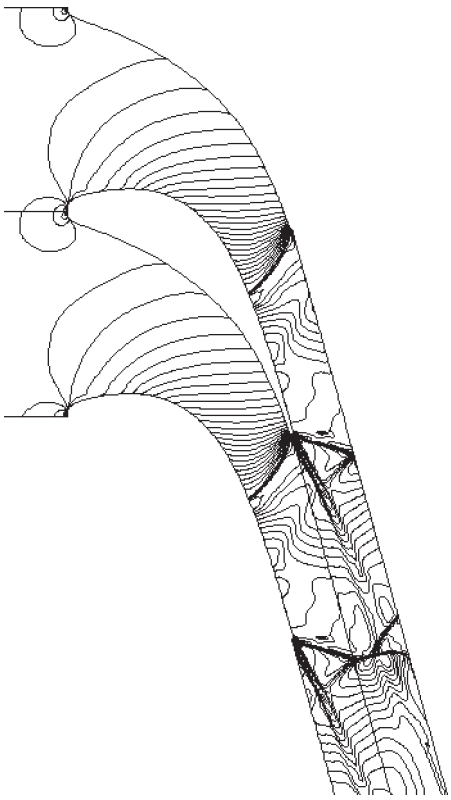

Figure 10. Mach number contours

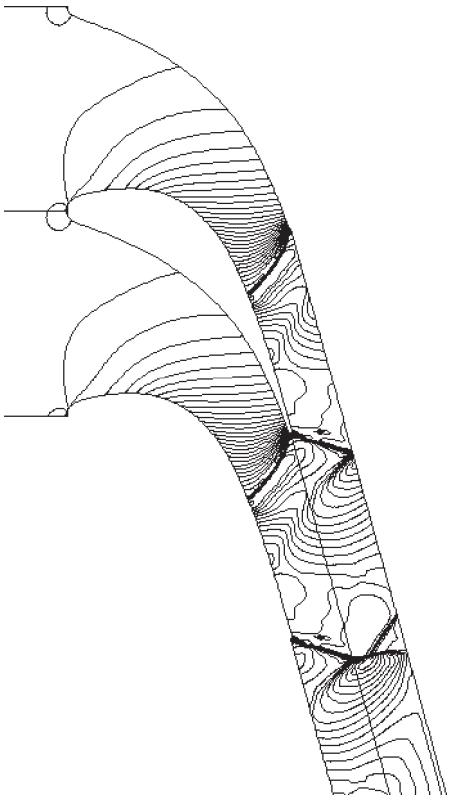

Figure 11. Pressure contours

for the spontaneous condensation (expansion rate, saturation rate *etc.*). Figure 14 shows the pressure deviation from the equilibrium due to condensation at the hub section.

As a result of spontaneous condensation, entropy increases. This increase is a measure of losses, which are the largest close to the blade hub and rapidly decrease along the blade length. Thus, the maximum change of the flow kinematic is observed by the blade hub. The liquid phase here is in the form of fog with a large number of small droplets. The outlet angle of the steam in $\Theta - x$ (circumferential-axial) plane for the diabatic flow was lower than that of the adiabatic flow along the whole blade length (the maximum departure, about 3%, was close to the blade hub), whereas the outlet angle in $r - x$ (radial-axial) plane for diabatic flow was lower than that of adiabatic flow from the hub to mid-span, and higher from the mid-span to the tip.

The erosion caused by the wet steam flow reduces the efficiency of the last stage rotor blades of a condensing steam turbine and makes their life shorter. Because of impingement of the water droplets on the rotor blade surface rotating with high speed, erosion damage on the suction side close to the leading edge takes place. The calculations (Figure 15) show the significant increase of the mean droplets radii close to the blade tip at the outlet of the stator and also the rapid reduction of the number of droplets along the blade length. This type of numerical calculation can determine the concentration and size of the droplets in

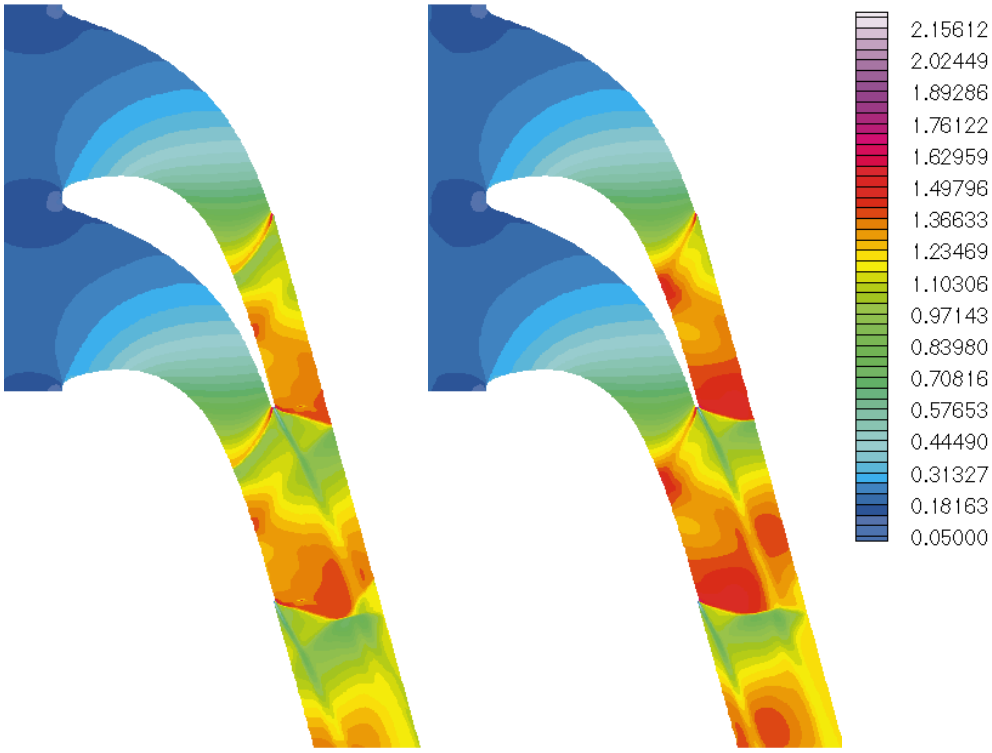

Figure 12. Mach number for a diabatic (left) and adiabatic (right) flow

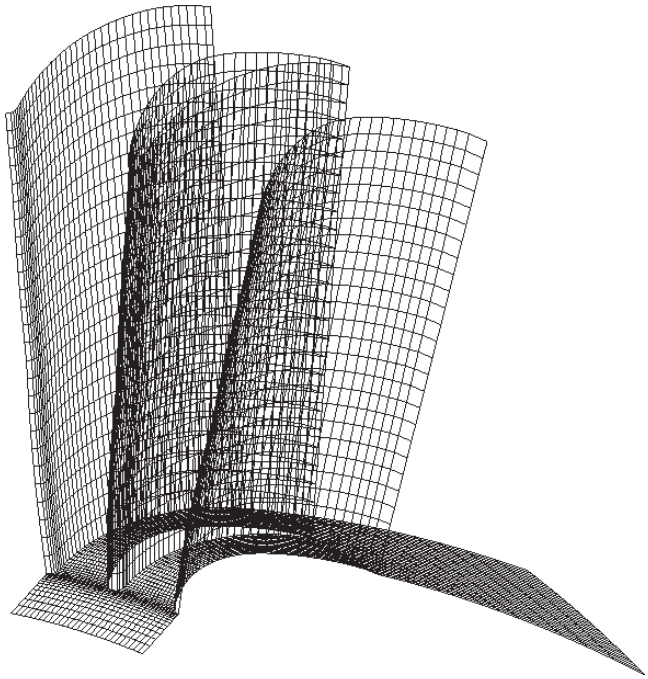

Figure 13. Geometry of the stator ($r_{hub} = 0.6715\,\mathrm{m}$, $r_{tip} = 1.430\,\mathrm{m}$)

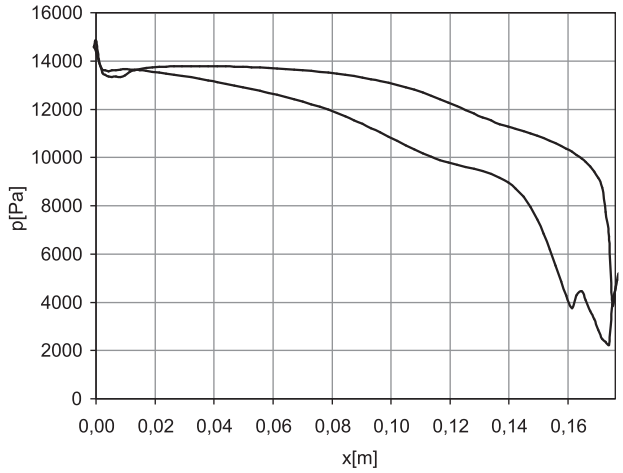

Figure 14. Pressure distribution on the profile in the hub section

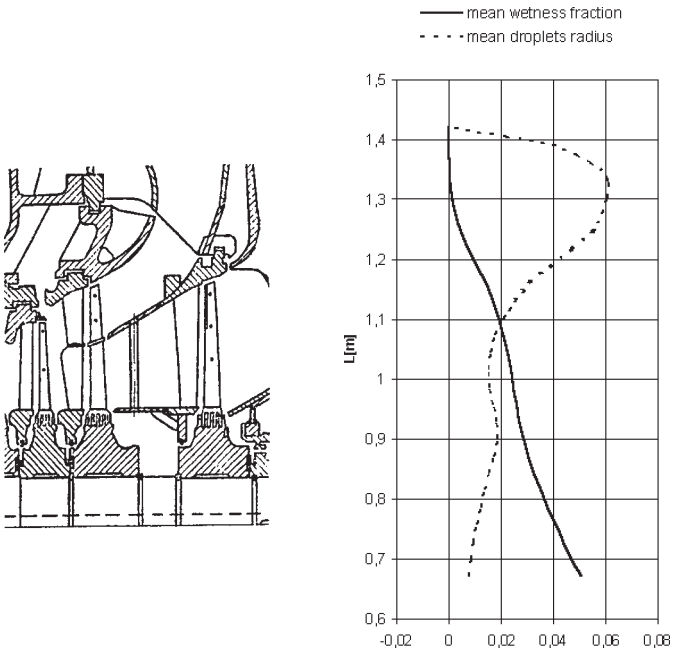

Figure 15. Distribution of mean values of the wetness fraction and droplets radii [μm] along the blade length at the outlet from the stator

3D space, *e.g.* at the inlet to the rotor. It helps to predict the location and intensity of the rotor blade erosion and is helpful for the calculations of material erosion.

4. Conclusions

There is no doubt that the homogeneous and heterogeneous nucleation in LP turbine stages is a very complex problem from the physical and computational point of view. Many theoretical and numerical problems have already been solved. Concluding, it shall be noted that in real LP steam turbines (last two stages):

- the flow is strongly 3D, which means that the 2D calculations are a significant simplification,
- the working medium is a real gas, thermally and calorically non-perfect,
- nucleation phenomenon depends on unsteady phenomena like rotor/stator interaction, turbulent and wake effects,
- the assumption of the no-slip model seems to be too general, while the size of the droplet rises along the blade length and prediction of the rotor tip erosion demands a different speed for the liquid phase.

In the numerical calculation of the steam flow through the last stages of LP turbines the real gas equation of state has to be used. The use of "local" real gas equation of state gives an accurate result for steam parameters and is not so time consuming. The presented model of inviscid flow gives correct results for the steam flow with homogeneous and heterogeneous condensation. On the basis of such calculations we can predict: the losses (Δh, Δs,...), the change of flow kinematic and the places of blade erosion.

It is worth noticing that many authors, like Schnerr [6], White [14, 15], Stastny [4], Bakhtar [2] *etc.*, who are strongly engaged in the numerical calculations of the steam condensing flow use different correction factors and parameter relations for the droplet growth equation and nucleation rate, thought the flow is governed by the same equations. The condensation phenomenon is so sensitive to flow parameters (pressure, temperature, *etc.*), that even their small changes cause significant changes in location and intensity of condensation. Therefore the use of accurate equation of state is so important. The skill of manipulating the various correction factors (see Equations (18) and (30)) is very useful and allows one to obtain a correct location and intensity of the condensation even with the help of the Hertz-Knudsen droplet growth equation [3].

Acknowledgements

I would like to express my gratitude to the "NATO Fellowship Programme" for supporting the common research with prof. G. H. Schnerr, who is an authority on the calculation of the condensing flows. I want to thank my teacher prof. T. Chmielniak for his kindness and understanding.

References

[1] Hill P G 1966 *J. Fluid Mech.* **25** (3) 593
[2] Bakhtar F and Mohammadi Tochai M T 1980 *Int. J. Heat and Fluid Flow* **2** 1
[3] Dejc M E and Filippov G A 1987 *Dvukh-faznye techenya*, Moscow
[4] Stastny M, Sejna M and Jonas O 1997 *Modelling the Flow with Condensation and Chemical Impurities in Steam Turbine Cascades* 2^{nd} European Conference on Turbomachinery-Fluid Dynamics and Thermodynamics, Antwerpen
[5] Stastny M and Sejna M 1999 *Numerical Analysis of Hetero-homogeneous Condensation of the Steam Flowing in Turbine Cascade* IMechE C557/082, pp. 815–826
[6] Schnerr G H and Winkler G 2001 *Unsteady Turbulent Multiphase Flow in Large Steam Turbines-Viscous/Inviscid Interactions in Transonic Axial Cascades* ASME Fluid Engineering Division Summer Meeting, New Orleans
[7] Winkler G 2000 *Laufrad-Leitrad-Wechselwirkung in homogen-heterogen kondensierenden Turbinenströmungen* Fakultät für Maschinenbau, Universität Karlsruhe (TH)
[8] Frenkel J 1955 *Kinetic Theory of Liquids* Dover Publ., New York
[9] Wagner W *et al.* 2000 *The IAPWS Industrial Formulation 1997 for the Thermodynamic Properties of Water and Steam* Transactions of the ASME, Journal of Engeneering Gas Turbines and Power **122** pp. 150-181

[10] Vukalovich M P and Rivkin C L 1969 *Teploenergetika* **3** 60 (in Russian)
[11] Górski J 1997 *Modelling of Real Gas Properties and Its Thermal-Flow Processes* Oficyna Wydawnicza Politechniki Rzeszowskiej, Rzeszów (in Polish)
[12] Kantrowitz A 1951 *J. Chem. Phys.* **19** 1097
[13] Moheban M and Young J B 1984 *A Time-marching Method for the Calculation of Blade-to-blade Nonequilibrium Wet Steam Flows in Turbine Cascades* IMechE, Conference on Computational Methods in Turbomachinery Paper C76/84, pp. 89 – 99
[14] White A J and Young J B 1993 *J. of Propulsion and Power* **9** 579
[15] White A J, Young J B and Walters P T 1996 *Phil. Trans. R. Soc. Lond. A.* **354** 59
[16] Godunov S K 1959 *Mat. Sbornik* **47** 271 (in Russian)
[17] Chmielniak T J, Wróblewski W and Dykas S 1997 *Archives of Thermodynamics* **18** (1-2) 99
[18] Wróblewski W 2000 *Numerical Simulation of Flow Phenomena in Heat Turbines* Zeszyty Naukowe Politechniki Śląskiej, Energetyka **132** (in Polish)
[19] Heiler M 1999 *Instationäre Phänomene in homogen/heterogen kondensierenden Düsen-und Turbinenströmungen* Dissertation, Fakultät für Maschinenbau, Universität Karlsruhe (TH)